spectively. The uncertainty assigned takes account of correlated errors.

Figure 11 is a plot of D_-^b versus pion energy, as obtained by Schnitzer and Salzman[4] and by Puppi and Stanghellini.[3] With the uncertainty assigned, the values of D_-^b obtained in the present experiments agree with the theoretical curves of Schnitzer and Salzman, and Puppi and Stanghellini and the considerations of Noyes and Edwards.[14] It, therefore, appears that the experimental results for the absolute value of the real part of

the forward-scattering amplitude are now in agreement with the theoretical values obtained by use of dispersion relations.

ACKNOWLEDGMENTS

Recoil Study of the Reaction $Al^{27}(p,3pn)Na^{24}$*

A. M. POSKANZER, J. B. CUMMING, AND R. WOLFGANG†

Chemistry Department, Brookhaven National Laboratory, Upton, New York

(Received 15 August 1962)

In order to study the mechanism of a simple spallation reaction induced by GeV-energy protons, measurements were made of the momentum properties of Na^{24} nuclei produced from an aluminum target. Data were obtained on: (1) the fraction of Na^{24} nuclei recoiling out of targets thick with respect to the range of the recoils (the targets were oriented both perpendicular and parallel to the proton beam); (2) the distribution of Na^{24} ranges from a thin target measured with plastic catchers subtending an angle of 2π; (3) the angular distribution of the Na^{24} recoils with respect to the beam. Results of Monte Carlo knock-on cascade and evaporation calculations for 0.36- and 1.8-GeV bombarding energies are compared with the data in the laboratory system. The calculations predict sharper sideways peaking in the angular distributions, and more momentum deposition at the higher bombarding energy, than are observed. The experimental data are also reduced to a set of velocity vectors which is then interpreted in terms of a simple, constant-deposition-energy mechanism in which the incident proton makes only one quasi-elastic collision with a single nucleon which does not escape from the nucleus. This treatment accounts for most of the data but also predicts a much larger sideways peaking in the angular distribution than is observed.

INTRODUCTION

THE basic model of high-energy nuclear reactions,[1] that of a nucleonic cascade followed by nuclear evaporation, has been used in various degrees of refinement to calculate cross sections of spallation reactions. However, the recoil momentum of the residual nucleus should be more sensitive to the mechanism of formation than measurements of only the formation cross section. For this reason the present recoil measurements were undertaken and compared with the predictions of various forms of the basic high-energy reaction model.

The recoil properties of Na^{24} produced by bombardment of aluminum with protons had been studied by Hintz[2] up to 90 MeV, by Fung and Perlman[3] up to 340 MeV, by Volkova and Denisov[4] and Crespo[5] at 660 MeV, and by Wolfgang and Friedlander[6] up to 2.2

GeV. All of these experiments were measurements of the fraction of Na^{24} recoiling out of an aluminum target thick compared to the range of the recoils. The present experimental work extends these measurements and presents more detailed experiments on thin targets to obtain information on the angular distribution and differential range of the recoils.

The ideal radiochemical recoil experiment, which would give the most information about the momentum of the recoil, would be a differential range measurement at many different angles to the beam. However, because of the limitations of beam intensity and time, less detailed experiments have been done. The thick-target experiments, the easiest to perform and the only kind extensively studied in the past, measure average momenta projected along a particular axis. The more detailed 2π differential-range curves measure the distribution in magnitude of the momenta averaged over angle. The angular distribution measurements, integrate over all momenta at a particular angle.

Two approaches have been used in the interpretation of the recoil data. The first is based on Monte Carlo knock-on cascade calculations[7] which kept track of the

* Research performed under the auspices of the U. S. Atomic Energy Commission.

† Present address: Yale University, New Haven, Connecticut.

[1] J. M. Miller and J. Hudis, Ann. Rev. Nucl. Sci. 9, 159 (1959).

[2] N. M. Hintz, Phys. Rev. 86, 1042 (1952).

[3] S. C. Fung and I. Perlman, Phys. Rev. 87, 622 (1952).

[4] V. Volkova and F. P. Denisov, J. Exptl. Theoret. Phys. (U.S.S.R.) 35, 538 (1958).

[5] V. P. Crespo, University of California Radiation Laboratory Report UCRL 9683, 1961 (unpublished).

[6] R. Wolfgang and G. Friedlander, Phys. Rev. 94, 775 (1954).

[7] N. Metropolis, R. Bivins, M. Storm, A. Turkevich, J. M. Miller, and G. Friedlander, Phys. Rev. 110, 185 (1958); N.

TABLE I. Percent loss from 1.716-mg/cm² Al.

GeV	F	B	P	Reference
28	10.1±0.2	4.5±0.1		This paper
2.9	10.7±0.2	4.0±0.1	7.6±0.1	This paper
2.25	10.1±0.4	3.8±0.2	7.7±0.4	a
1.6	11.2±0.2	3.7±0.1	7.8±0.1	This paper
1.6	11.0±0.1	3.4±0.1		a
1.0	11.7±0.6	3.4±0.2		a
0.8	13.1±0.2	3.2±0.1	7.9±0.1	This paper
0.8	12.4±0.1	2.9±0.1		a
0.5	13.7±0.1	2.6±0.1		a

a See reference 6.

momenta. An evaporation calculation has been added and the final recoil momentum in the laboratory system compared directly with experiment. The agreement is poor and improvement is difficult because, at present, a computer program is not available for optimum fitting of the input parameters. Therefore a second approach has been adopted. The experimental data on the momentum of the recoil have been reduced to a set of vectors[8,9] characterized by a number of parameters sufficient to describe the data. The parameter fitting starts with the most detailed experiments so that the results may be used to help fit the less detailed experiments. Finally, the parameters of the vector analysis are interpreted in terms of a simple mechanism consistent with the basic cascade-evaporation model.

THICK-TARGET EXPERIMENTS

In these experiments, targets thick compared to the ranges of the recoils are exposed perpendicular to the beam, and the fractions of the activity that recoil out both in the forward and backward directions are measured and designated F and B, respectively. In separate experiments targets are oriented at 10° to the beam and the total fraction that recoils out is measured. This quantity divided by two is designated P. When these quantities are multiplied by W, the target thickness, the products represent average effective ranges in the forward, backward, and perpendicular directions, respectively. As long as W is greater than the maximum range, F, B, and P are inversely proportional to W.

In the present experiments 0.00025-in. Al targets were used with 0.00025-in. Mylar catcher foils protruding slightly beyond the leading edge of the target. Other Mylar foils were always added to measure their activation blank. This was small if the foils were washed and degreased before irradiation and kept free of fingerprints. The relative counting efficiency of the target and catcher foils was measured for the particular geometry used. The data are shown in Table I together with the unpublished results of Wolfgang and
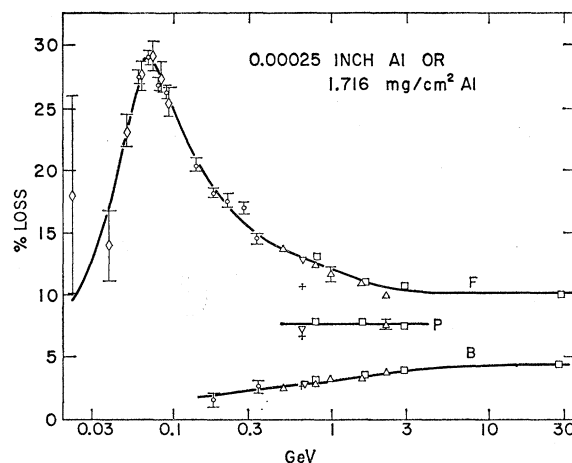

FIG. 1. The percent of the Na²⁴ recoiling out of 0.00025-in. Al in the forward, perpendicular, and backward directions as a function of proton bombarding energy. The various experimenters are as follows: ◊ Hintz (reference 2); ○ Fung and Perlman (reference 3); + Volkova and Denisov (reference 4); ▽ Crespo (reference 5); △ Wolfgang and Friedlander (reference 6); □ this work.

Friedlander.[6] These, and all of the previously published data, are plotted in Fig. 1. Except for the point of Volkova and Denisov[4] the agreement between the various experimenters is good. Some qualitative features are of interest. The curve for F rises from threshold to 70 MeV, indicative of the large momentum transfer of a compound-nucleus type reaction.[10] The fall off at higher energies was attributed by Fung and Perlman[3] to the onset of nuclear transparancy. They found that the data from 80 to 340 MeV could be interpreted in terms of constant deposition energy for those knock-on cascades that would lead to Na²⁴. For constant deposition energy the reason that the deposition momentum decreases initially as $E^{-1/2}$ with increasing bombarding energy can be seen from the simple classical expression $\Delta p \propto E^{-1/2}\Delta E$ (derived from $p^2=2mE$). The relativistic extension of this formula predicts the flattening out at higher bombarding energies.

2π DIFFERENTIAL-RANGE EXPERIMENT

To obtain information about the distribution in ranges of the recoils, a thin-target, thin-catcher experiment was performed with 2.9-GeV protons. The catchers were Formvar plastic, about 90 μg/cm² thick. They were larger than the target and practically in contact with it, so as to subtend an angle of 2π from the target. The target was 1 cm square, 38 μg/cm² thick, on a 0.00025-in. Mylar backing. Two targets were used back to back, as illustrated at the bottom of Fig. 2, so as to measure both the forward and backward recoils in the same experiment. The 0.00025-in. Mylar foils at the end of the stack were placed so as to insure a measurement of the activation blank of both the Formvar and the Mylar.

Metropolis, R. Bivins, M. Storm, J. M. Miller, G. Friedlander, and A. Turkevich, ibid. 110, 204 (1958).

[8] N. Sugarman, M. Campos, and K. Wielgoz, Phys. Rev. 101, 388 (1956).

[9] N. T. Porile and N. Sugarman, Phys. Rev. 107, 1410 (1957).

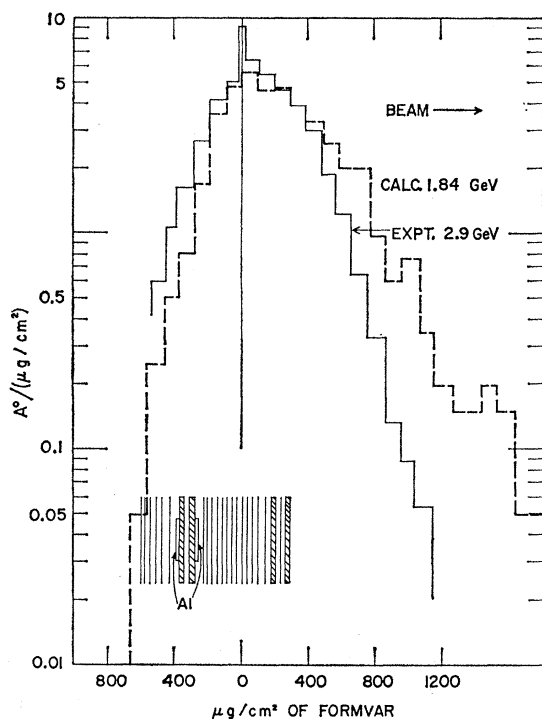[10] A. M. Poskanzer, following paper [Phys. Rev. 129, 385 (1963)].

FIG. 2. Experimental results of the 2π differential-range experiment. The ordinate is the Na^{24} activity one day after irradiation of each catcher foil divided by the thickness of the foil. The abscissa is the distance along the beam direction from the midpoint of the target. Insert at the bottom shows the target arrangement. The thick foils are 0.00025-in. Mylar. Dashed curve is the result of the Monte Carlo calculation.

TABLE II. Target parameters for angular distribution experiments.

	0.38 GeV	2.2 GeV	2.2 GeV (recent)
Target area	$\frac{1}{4}$ in.$\times\frac{1}{4}$ in.	$\frac{1}{2}$ in.$\times\frac{1}{2}$ in.	$\frac{1}{2}$ in.$\times\frac{1}{2}$ in.
Collection radius	$\frac{15}{16}$ in.	$3\frac{1}{2}$ in.	6 in.
Height of collection strip	$\frac{3}{8}$ in.	$1\frac{1}{2}$ in.	$1\frac{9}{16}$ in.
Target thickness	27 μg/cm^2	27 μg/cm^2	22 μg/cm^2
Target backing thickness	1 mg/cm^2	1 mg/cm^2	20 μg/cm^2
Collection interval	30°	30°	15°

with 2.2-GeV protons and at the Nevis synchrocyclotron with 0.38-GeV protons. The experiment at 2.2 GeV was repeated recently with better statistics and an improved apparatus which is shown in Fig. 3. The dimensions of all three recoil catchers are given in Table II. As the Cosmotron beam spiraled inwards after acceleration to full energy in the most recent experiment, it first made several hundred traversals through the target, then passed through a $\frac{1}{8}$-in.-Lucite lip, and a $\frac{3}{8}$-in.-brass block just downstream from the target so as to jump[12] the beam past the catcher foils to lower their activation blank. The beam jumper was encased in paraffin so as to prevent recoils from it from reaching the catcher foils. In the earlier Cosmotron experiment the catcher foils were shadowed by a brass block in a separate straight section of the accelerator. In the synchrocyclotron experiment a graphite block one inch downstream from the apparatus prevented the beam from making many traversals through the catcher foils. These foils con-

All the foils were mounted on horseshoe-shaped Mylar frames 0.008 in. thick. The assembled target was positioned on the pneumatic ram at the Cosmotron, and the full-energy beam allowed to spiral into the target through the open end of the frames. The thickness of each Formvar catcher was measured with an alpha-particle thickness gauge.[10,11] The net Na^{24} activity of each foil divided by its thickness is shown in Fig. 2. The forward and backward catchers were normalized to each other by summing the Na^{24} produced from each target. The activity that remained in the Al layer (highest point in Fig. 2) is quite uncertain, because in this type of target arrangement it is obtained as a small difference between two large numbers. Because of the 2π nature of this experiment it is necessary to know the angular distribution and to differentiate the data to obtain a conventional differential range curve. This is shown in a later section.

ANGULAR-DISTRIBUTION EXPERIMENTS

Experiments to measure the angular distributions of Na^{24} recoils produced from aluminum targets were originally performed at the Brookhaven Cosmotron
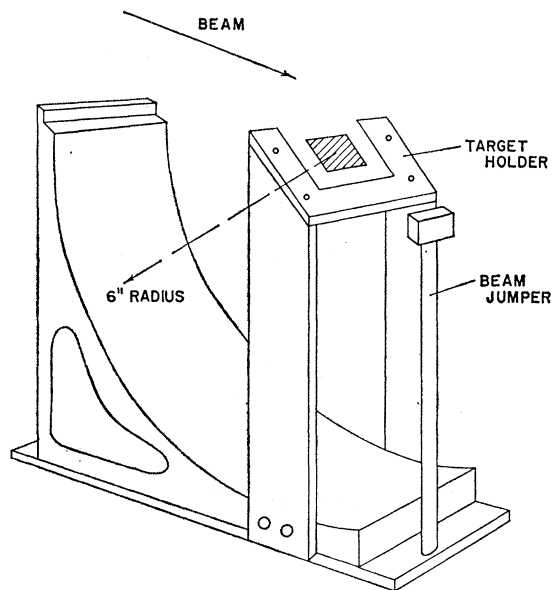

FIG. 3. Apparatus used for measuring the angular distribution of the recoils. The recoils are collected on plastic foils at a 6-in. radius from the target.

[11] K. Ramavataram and D. I. Porat, Nucl. Instr. and Methods 4, 239 (1959).

[12] O. Piccioni, D. Clark, R. Cool, G. Friedlander, and D. Kassner, Rev. Sci. Instr. 26, 232 (1955).

TABLE III. Intensity per unit solid angle in the laboratory system, $F_L(\theta_L)$, vs laboratory angle at the midpoint of the collection interval, θ_L.

θ_L (deg) \ GeV	0.38	2.2	2.2 (recent)
15			1.37
30	2.07	1.37	1.38
45			1.29
60	1.50	1.30	1.30
75			1.21
90	0.80	1.03	1.07
105			0.89
120	0.46	0.72	0.71
135			0.60
150	0.35	0.55	0.53
165			0.49

sisted of several layers of plastic strips, usually 0.00025-in. Mylar. The second layer, beyond the maximum range of the Na²⁴ recoils, was used to measure the Mylar activation blank. Even with these precautions, recoils could not be measured at less than 15° to the beam in the earlier experiments, and at less than $7\frac{1}{2}°$ to the beam in the more recent experiment. To normalize the data these contributions were estimated by extrapolation. In the recent experiment two bombardments were performed, one looking at the forward recoils, one looking at the backward recoils, with overlap at the 90° point. In the earlier experiments the ratios of the activities of only a few foils at a time were studied so that the collection angles did not differ by more than ±45° from the normal to the target. The normalized data, $F_L(\theta_L)$, are given in Table III. This is the angular distribution per unit solid angle in the laboratory system, normalized so that

$$\sum 2\pi F_L(\theta_L)\langle\sin\theta\rangle_{av}\Delta\theta = 4\pi. \tag{1}$$

It can be seen that the data of the more recent experiment at 2.2 GeV are in excellent agreement with those of the earlier experiment indicating that the thick target backing and poorer resolution of the earlier experiment had no significant effect. The data of the 0.38-GeV experiment and the recent 2.2-GeV experiment are also plotted in Fig. 4 and will be discussed in the succeeding section.

MONTE CARLO CALCULATION

When the most recent knock-on cascade calculations[7] were being programmed for the Maniac computer it was not thought that they would be used to calculate recoil momenta and the sign of one of the three direction cosines of each cascade particle was not recorded. However two special cascade calculations were kindly performed by R. Bivins for 1.84- and 0.36-GeV protons on aluminum. For the two cascade particles resulting from the first collision, the signs of this direction cosine were chosen to be opposite, and for the remaining collisions randomly. All of the other assumptions remained the same and are described in detail in the papers.[7] By summing the momenta of all incoming and outgoing
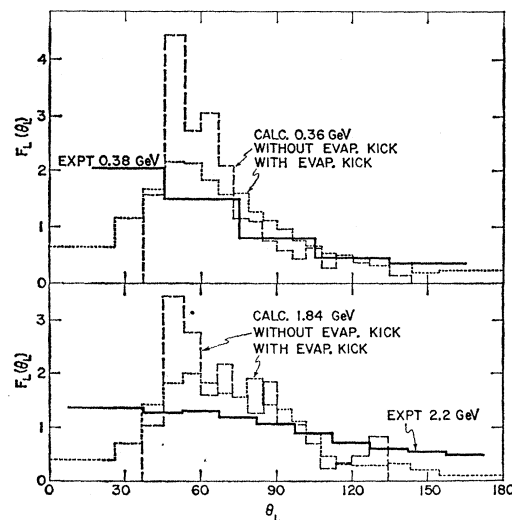

FIG. 4. Angular distributions per unit solid angle of the recoils in the laboratory systems. Solid curves are experimental. The other curves represent results of Monte Carlo calculations.

particles, the momentum of the recoil was calculated for each knock-on cascade. Those cascades which would lead to mass-24 products by subsequent evaporation were then selected on the basis of the mass and deposition energy of the cascade product, as indicated in Table IV. The fraction of events assigned to each mass number by these criteria at each energy are also indicated. At both energies, mass 25 and 26 intermediates are the major contributors, with mass 25 more favored at 1.8 GeV.

For each cascade product thus selected, an estimate of the contribution to the final momentum from the evaporation process was made in a second Monte Carlo calculation. Here a constant-temperature Maxwellian spectrum of the energies of the evaporated particles was assumed. The temperature was calculated with a level-density parameter, $a = 2.7$ MeV⁻¹, and an average binding energy of 9 MeV per nucleon was assumed. The calculation was not a completely valid evaporation calculation since the number of particles evaporated was selected beforehand. This limits somewhat the number of both the very-high- and very-low-energy particles emitted, but is thought not to be very serious in light of later discussions. At 1.84 GeV five evaporation cascades were performed for each of the 174 knock-on cascades

TABLE IV. Mass number, deposition energy, and frequency of selected Monte Carlo cascades.

Cascade product		Fraction of selected events (in %)	
Mass	Deposition energy (MeV)	at 0.36 GeV	at 1.8 GeV
24	0–9	1	4
25	9–24	40	61
26	24–41	48	33
27	41–58	11	2

TABLE V. Comparison between experiment and calculation for the percentage of Na^{24} recoiling out of 0.00025-in. Al.

	0.36 GeV		1.84 GeV	
	Calc.	Expt.	Calc.	Expt.
F	12.6	14.7	17.2	10.9
B	1.7	2.4	2.4	3.5
P	8.2	(≈ 8)	14.9	7.7

available, and at 0.36 GeV three evaporation cascades were performed for each of the 757 knock-on cascades.

For comparison with the thick-target experiments the calculated recoil momenta were converted to ranges[10] in Al. The quantity FW was taken to be the sum of the projections along the beam axis of the ranges of the forward recoiling nuclei divided by the total number of recoils (including the backward recoiling ones). The other quantities were defined similarly. In Table V the calculated values of F, B, and P for a 1.716-mg/cm² target are compared with the experimental ones from Fig. 1. The agreement at the lower bombarding energy is fairly good. At the higher bombarding energy the agreement is poor, especially for the value of P. Also the direction of the variation of F with bombarding energy is not reproduced. It was verified that the calculated contribution of the evaporation stage was not very different at the two bombarding energies, and thus the larger predicted ranges are due to larger momentum which should, according to the Monte Carlo calculation,

FIG. 5. (a) Diagram of the vectors used in fitting the data. The quantities $v_{||}$ and $v_{\perp}$ are the components of v parallel and perpendicular to the beam. The vector v is called the knock-on kick, the vector V, the evaporation kick. (b) The angles θ and θ_L are the angles of the recoil with respect to the beam in the system of the struck nucleus and laboratory system, respectively. This diagram is for the case where V accidently lies in the $v_{||}-v_{\perp}$ plane.

be imparted in the knock-on phase at the higher bombarding energy. Obviously this prediction is not borne out experimentally.

For comparison with the 2π differential range curve the momentum distribution from the Monte Carlo calculation was converted to range in Formvar and projected along the beam axis. This is shown as the dashed histogram in Fig. 2. Unfortunately, the experiment was done at 2.9 GeV while the calculation is for 1.8 GeV and, as can be seen in Fig. 1, one would expect slightly more forward motion at the lower bombarding energy. However, there still appears to be some discrepancy as was shown by the average forward and backward ranges of Table V.

It is the angular distributions that exhibit the most dramatic discrepancies between experiment and calculation. The angular distributions of the recoil momenta from the Monte Carlo calculations are plotted together with the experimental data in Fig. 4. It is seen that the calculation predicts strong sidewise peaking that is only partially smeared out by the evaporation kick. No evaporation kick of reasonable magnitude will bring the calculation into agreement with experiment. To see if the criteria for choosing those knock-on cascades that would lead to mass 24 could cause the discrepancy, the results of the calculation were sorted according to the mass of the knock-on product. All the distributions were similar in that they all showed a sharp drop in the forward direction. At the lower bombarding energy the angular distributions resulting from mass-25 and mass-26 knock-on products were further divided in two groups each, according to deposition energy. No differences were apparent, indicating that a small change in the choice of the deposition energies would not affect the results. Also, the unreasonable assumption was made that all the mass-26 cascades resulted in deuteron emission, and even then the dip in the forward direction only partially disappeared. Thus it is concluded that the present knock-on cascade calculations predict too strong a sideways peaking for products of this fairly simple, low-deposition-energy reaction on aluminum. Without doing further calculations it is difficult to tell which assumptions or details of the Monte Carlo cascade calculation cause the discrepancy. However, it is suggested that the neglect of refraction and of the recoil of the nuclear potential when nucleons cross its boundary[13] might be causes of the discrepancy.

VECTOR ANALYSIS

In order to make further progress in analyzing the experimental data it was decided to fit the recoil data to a set of vectors[8,9] consistent with the basic cascade-evaporation model. The vectors are shown in Fig. 5. The quantity v we will call the average velocity of the struck nucleus as a result of the knock-on cascade. Because we
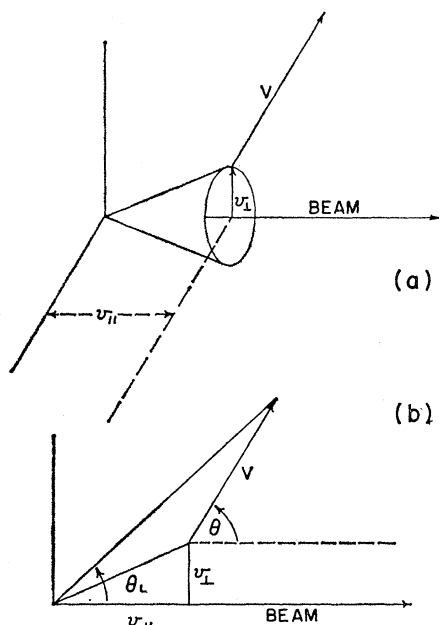
[13] N. T. Porile, Phys. Rev. 120, 572 (1960).

are not dealing with compound-nucleus reactions, the system of the struck nucleus is not the center-of-mass, nor is **v** necessarily directed along the beam axis. The quantity v_{11} is its component parallel to the beam axis, and $v_\perp$ its component perpendicular to the beam axis. In this moving system, the excited struck nucleus then evaporates particles. It is assumed that, on the average, the angular distribution of the evaporated particles in the system of the struck nucleus is symmetric about a plane perpendicular to the beam axis. Although the angular-momentum vector of a single struck nucleus may be at any angle, simple considerations show that for a large number of cascades there can be no net component along the beam direction. Thus, on the average, the angular distribution is symmetric about 90° to the beam direction. The average velocity imparted to the recoil in the system of the struck nucleus due to the evaporation of the light particles is designated **V**. As described, this vector may have an angular distribution consisting of even powers of $\cos\theta$ (see Fig. 5) and will be assumed to be simply of the form $a+b\cos^2\theta$. Thus, the parameters that we are going to use to fit the recoil data are the following: **v**, the knock-on kick, and its components parallel and perpendicular to the beam axis; V, the magnitude of the evaporation kick; and b/a, the parameter describing the anisotropy of the evaporation kick. Other symbols which will be useful in later discussions are $\eta=v/V$, $\eta_{11}=v_{11}/V$, and $\eta_\perp=v_\perp/V$. In this paper we are only concerned with values of η less than unity.

A phenomenon that does not fit into this framework easily is that of the recoil due to the momentum (Fermi motion) of the nucleons in the nucleus which are struck in the prompt cascade leaving "holes." The concept of average hole momentum is an artifice which allows one to consider the conservation of momentum in the collision of a bombarding particle with moving nucleons in terms of the two simpler separate problems: the collision with a stationary nucleon and the average momentum of the struck nucleons before the collision. At high bombarding energies the recoil due to this effect would tend to be symmetric about 90° to the beam[14] and would be included in the parameters V and b/a. At lower bombarding energies, because of the effect of relative velocity on cross section and the variation of the nucleon-nucleon cross sections themselves with energy, there may be a preference[14] for head-on versus overtaking collisions or vice versa, which would contribute to v_{11}. It should be pointed out that in the Monte Carlo calculations the hole-momentum effect is automatically included in the knock-on cascade part of the calculation when one does the calculation for a target of moving nucleons. Thus, one should not equate the momentum obtained from the knock-on cascade calculation with **v**. In fact, in the calculations of Porile[18] the recoil momenta observed in the backward direction probably arise from

the Fermi motion of the struck nucleons.[15] In the rest of this paper we will continue to describe **V** as the evaporation kick, and only in the last section consider the contribution of hole momentum to it.

ANGULAR-DISTRIBUTION ANALYSIS

First, the angular-distribution data will be analyzed so that the parameter obtained for the anisotropy of the evaporation step can be used to help fit the other recoil data. The other parameters, $\eta_{11}(=v_{11}/V)$ and $\eta_\perp(=v_\perp/V)$, determine the transformation of the angular distribution per unit solid angle from the laboratory system, $F_L(\theta_L)$, to $F(\theta)$ in the system of the struck nucleus:

$$F(\theta)=G(\eta_{11},\eta_\perp,\theta_L)F_L(\theta_L),\qquad(2)$$

where G is the transformation function. The quantity b/a, which determines the anisotropy of the evaporation step, is then obtained by fitting $F(\theta)$ with a normalized $\cos^2\theta$ distribution:

$$F(\theta)=\frac{1+(b/a)\cos^2\theta}{1+b/3a}.\qquad(3)$$

In the case where $\eta_\perp$, the sidewise knock-on kick, is zero, the transformation function is that of the standard center-of-mass transformation with η_{11} given by the equation:

$$F-B=\frac{1+(b/3a)\eta_{11}^2}{1+b/3a}\eta_{11},\qquad(4)$$

where F is the fraction of recoils emitted into the forward laboratory hemisphere, and B that into the backward hemisphere.[16] It can be shown[17] that the existence of the sidewise knock-on kick, $\eta_\perp$, does not affect this equation so that the forward-backward shift in the laboratory system may still be used to obtain η_{11} from the data. However the angular-distribution transformation function is more complicated because of the averaging necessitated by the fact that the vector **V** originates from any point on the rim of the base of the cone in Fig. 5(a). The following expansion for $1/G$ in powers of $\eta_\perp$ has been obtained:

$$G^{-1}(\eta_{11},\eta_\perp,\theta_L)=G_0^{-1}(\eta_{11},\theta_L)$$
$$-\tfrac{1}{4}\eta_\perp^2(3\cos^2\theta_L-1)+T(\eta_\perp^4),\quad(5)$$

where the term $T(\eta_\perp^4)$ denotes terms of the order of $\eta_\perp^4$ and higher. The quantity $G_0(\eta_{11},\theta_L)$ is the standard transformation function[18] for $\eta_\perp$ equal to zero. The angles

[14] L. Winsberg and T. P. Clements, Phys. Rev. **122**, 1623 (1961).

[15] In the present vector model, v_{11} is the algebraic average component of **v** along the beam, and any negative values of **v** subtract twice from the average. However, since in this model at high energies most of the hole momentum is included in **V** and not **v**, this effect is expected to be small.

[16] L. Winsberg, University of California Radiation Laboratory Report UCRL-8618, 1958 (unpublished), p. 44.

[17] B. Foreman (private communication).

[18] E. g., J. B. Marion, T. I. Arnette, and H. C. Owens, Oak Ridge National Laboratory Report ORNL-2574, 1959 (unpublished).
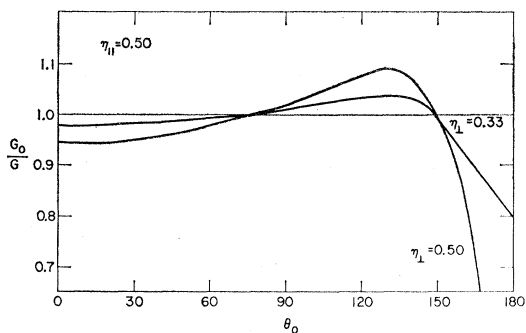
FIG. 6. Graph constructed using Eqs. (5) and (6) illustrating the effect of $\eta_\perp$.

transform as follows:

$$\cos\theta = \cos\theta_0 - \tfrac{1}{2}\eta_\perp^2(1 - \tfrac{1}{2}\cos\theta_L \sin^2\theta_L) + T(\eta_\perp^4), \quad (6)$$

where θ_0 is the angle which corresponds to G_0.

To illustrate the effect of $\eta_\perp$ (which arises from the sidewise knock-on kick), the quantity G_0/G has been plotted in Fig. 6 for some representative values of η_{11} and $\eta_\perp$. The quantity plotted is equal to $F_L(\theta_L)G_0$ when b/a is zero. Figure 6 illustrates the effect of neglecting $\eta_\perp$ in the transformation. One might say then that the effect of $\eta_\perp$ on the angular distribution is to cause a dip in the backward direction. One can visualize that for η_{11} equal to zero and $\eta_\perp$ greater than unity, the distribution of recoils assumes a toroidal shape. For $\eta_\perp$ less than unity the effect of η_{11} is to emphasize the dip in the backward direction and deemphasize that in the forward direction.

The mechanics of transforming the experimental angular distributions was as follows. The value at 90° was divided by interpolation so that the fraction going into each of the laboratory hemispheres, F and B, could be obtained. Using Eq. (4) and estimates of b/a obtained below by successive approximations, the values of η_{11} shown in Fig. 7 were obtained. The errors on η_{11} reflect the errors in the data and the various extrapolations and interpolations. From η_{11}, the values of G_0 averaged over the proper intervals were obtained. The values of $\eta_\perp$ were estimated so as to try to make the final distributions, $F(\theta)$, calculated by Eqs. (5) and (6), symmetric about 90°.

In Fig. 7 the vertical widths of the rectangles reflect the errors in η_{11}. The smooth curves are drawn with the indicated values of b/a. A rise in the backward direction, especially significant at 0.38 GeV, is observed. Even with $\eta_\perp$ set equal to zero this is apparent, which is just the opposite behavior from what one would expect from Fig. 6. The values of $\eta_\perp$ used were chosen consistent with the analysis of other data in a later section. The errors in $\eta_\perp$ in Fig. 7 top and middle indicate that little information concerning $\eta_\perp$ is obtained. Figure 7 bottom shows the analysis done both with $\eta_\perp$ equal to zero and 0.3, again indicating the small sensitivity to $\eta_\perp$ for small η. If the sidewise kick of the knock-on step were as large as predicted by the Monte Carlo calculations described

earlier, then the effect of $\eta_\perp$ would be quite pronounced.

It was thought that two experimental effects might possibly explain the observed rise in the backward direction and obscure the dip predicted by this type of analysis. One is the curvature of the recoils in the magnetic field which, of course, would be more severe in the cyclotron than in a straight section of the Cosmotron. However, the small collection radius of the cyclotron recoil catcher was chosen to reduce this effect to insignificant magnitude. The second effect is backscattering from the thick Mylar target backing used in the earlier experiments. Since in the laboratory system most of the recoils go forward (more so at 0.38 GeV than at 2.2 GeV) the effect of backscattering would have a larger percentage effect in the backward direction than in the forward direction. This is the main reason the experiment was repeated at 2.2 GeV with a thin Formvar target backing. However, apparently this had no effect on the results. It would be desirable to repeat the experiment at 0.38 GeV where the anomaly is pronounced and the effect of $\eta_\perp$ should be more significant.

Even though the experiments failed to measure any significant sidewise knock-on kick, $\eta_\perp$, it is clear, especially from Fig. 7 bottom that there is a small but definite negative anisotropy of the angular distribution of V, the evaporation kick. This anisotropy is a gross average over the distribution of angular momenta deposited and the various evaporation paths.
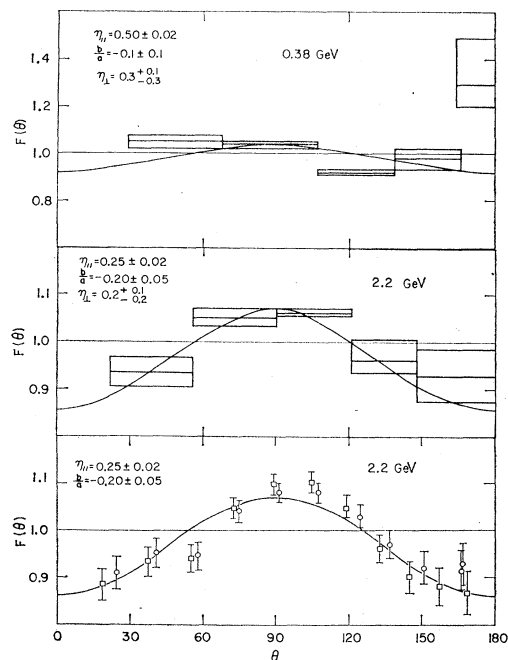

FIG. 7. Angular distributions of V, the evaporation kick, in the system of the struck nucleus, with respect to the angle of V to the beam direction. The curves are drawn with the indicated values of b/a. The errors indicate the range of values that will fit the data. The bottom graph represents the more recent experiment at 2.2 GeV. For the circles the analysis was done with $\eta_\perp$ equal to 0.3, for the squares, $\eta_\perp$ was zero.

DIFFERENTIAL-RANGE ANALYSIS

Now that we have some information on the anisotropy of V, one can do a vector analysis on the 2π differential-range data[19] shown in Fig. 2. However, because of the 2π nature of the experiment, one has to differentiate the data to obtain the spectrum of V. As the analysis is slightly complicated, a simple illustration may help. For recoils of a unique velocity, V, isotropic in the laboratory system, a plot similar to Fig. 2 would be a rectangle extending from $-R$ to $+R$ if one neglected straggling. The effect of b/a would cause the rectangle to bow in the center. Several values of V would give rise to a pyramid. The only effect of v_{II} would be to shift the curve forward if range is proportional to velocity. Since V is much larger than v_{II}, and since one expects a broad distribution in V from the random-walk summing of evaporation kicks, we have neglected the distribution of v_{II} in the analysis in comparison to the distribution in V.

The equation for the number of recoils stopping in a thickness dt as a function of t, distance along the beam axis, is

$$I(t,R)dt = \frac{P(R)dR}{2R}\frac{1}{1+b/3a}\left[1+\frac{b}{a}\left(\frac{t}{R}-\frac{v_{\text{II}}}{V}\right)^2\right], \quad (7)$$

where $P(R)dR$ is the probability of obtaining the value R in the interval dR. The assumption is made that over the interval from $V-v_{\text{II}}$ to $V+v_{\text{II}}$, range is proportional to velocity plus a constant. As seen in the following paper,[10] this is a good approximation except at the smallest ranges. To obtain the range-energy relationship in Formvar the average projected ranges in Formvar were calculated and compared with those in Al which were obtained from the thick-target experiments. It was found that the average range in Formvar divided by the average range in Al is 1.00 for the forward recoils and 0.91 for the backward recoils. To interpret the present experiment it was assumed that the Na^{24} ranges in Formvar are 0.95 times the ranges in Al presented in the next paper.[10]

A value of v_{II} corresponding to 0.26 (MeV)$^{1/2}$ was chosen[20] as best describing the forward shift of the symmetric part of Fig. 2. Based on the angular distribution experiments, the parameter b/a was chosen to be -0.2. It will be assumed that there are a discrete number of values of V equal to the number of foils in the experiment. The analysis, say for the forward catchers, proceeds by starting with the outermost foil. From the midpoint of the foil t_{max} is calculated. This represents the maximum depth penetrated for the largest value of V, and when converted to velocity is equal to $V+v_{\text{II}}$. Using the assumed constant value of v_{II}, V is calculated. From the intensity in the last foil Eq. (7) is used to calculate $P(R)\Delta R$. This is equal to $P(V)\Delta V$. The quantity ΔV is obtained from the end points of the foil

[19] The data are sensitive to $\eta_{\perp}$ only if the range-energy relationship deviates greatly from $R \propto V$, which is not the case here.

[20] The units are the square root of the kinetic energy.
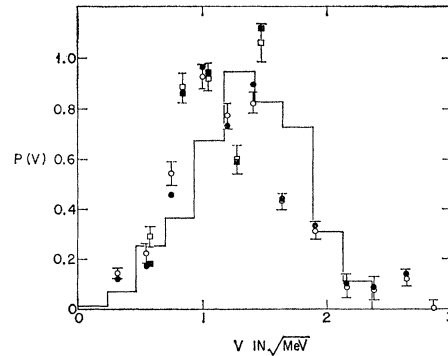

FIG. 8. Probability distribution of V, the evaporation kick. The abscissa is the square root of the energy of the recoil. The circles were obtained from forward recoils, squares from backward recoils. The open points were obtained assuming b/a is zero, the solid points assuming b/a equals -0.2. The histogram is the result of an evaporation calculation explained in the discussion section.

and the range-energy relationship. Thus one obtains $P(V)$ for the largest value of V. Equation (7) is used to obtain the intensity in the other foils resulting from the recoils with this value of V. After subtracting these values, the next-to-last foil is then analyzed as above. The values obtained for $P(V)$ are shown in Fig. 8. The scatter of the points appears to be a little larger than the internal errors would indicate. On the average, the points obtained from the backward catchers are not displaced relative to those from the forward catchers, indicating a reasonable choice for v_{II}. It can be seen that using the value of b/a obtained from the angular distribution experiments is not very critical to the analysis. The average value of V is 1.25 (MeV)$^{1/2}$. From the straggling curves presented in the following paper,[10] it can be seen that a monoenergetic recoil of this velocity would give rise to a curve about half as broad as that in Fig. 8. Thus, straggling is probably not a very important contributor to the curve. The curve will be interpreted in the discussion section.

ANALYSIS OF THICK-TARGET DATA

We now interpret the thick-target recoil data in terms of the vector analysis using the information obtained from the more detailed experiments. Equations derived by Sugarman[21] are used to calculate from the data average values of the parameters V, v_{II}, b/a, and $v_{\perp}$. The equations assume straight recoil paths and that range is proportional to the Nth power of the velocity. The

[21] N. Sugarman (private communication, 1961). Quoted in reference 5 on p. 21 for any value of N. For the value of $N=1.2$ used in this paper the equations reduce to the following:

$$F+B = (R/2W)[1+(b/6a)+\eta_{\text{II}}^2(1.23-0.31b/a)$$
$$+\eta_{\perp}^2(0.06+0.02b/a)],$$
$$F-B = (\eta_{\text{II}}R/W)(1.07+0.02b/a),$$
$$F+B-2P = (R/2W)[(b/4a)+\eta_{\text{II}}^2(1.17-0.29b/a)$$
$$-\eta_{\perp}^2(0.59+0.06b/a)].$$

The equations are complete to terms of the order of η_{II}^2, $\eta_{\perp}^2$, and b/a.
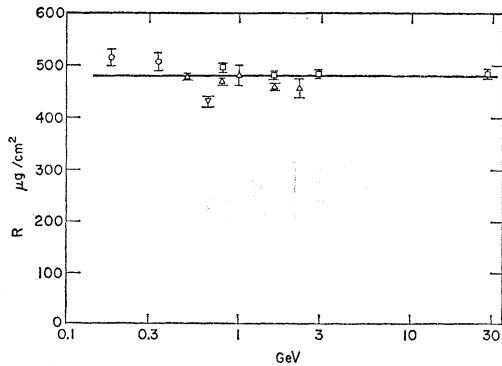
FIG. 9. The average range in Al corresponding to V, the evaporation kick, as obtained from thick-target experiments. The horizontal line at 480 μg/cm² is consistent with most of the data. The symbols are defined as in Fig. 1.

value of N of 1.2, as derived in the next paper,[10] is used although it will be shown that for $N=1$ the conclusions are little changed. On the basis of the angular-distribution measurements, it is assumed that $b/a=-0.1$ for bombarding energies below one GeV, and -0.2 for 1 GeV and above. Actually, only $\eta_\perp$ is sensitive to this assumption. Also V and η_{11} are not at all sensitive to $\eta_\perp$, thus making the analysis valid even for those cases where only F and B were measured. The results for R, the range which corresponds to V only (the evaporation kick), for η_{11}, and for $\eta_\perp$ are shown in Figs. 9, 10, and 11, respectively. The values of R are apparently constant over a very wide range of bombarding energies, even though at each bombarding energy there is a broad distribution as shown in the differential-range experiment. The average value is 480 μg/cm² of Al which corresponds to $V=1.32$ (MeV)$^{1/2}$. An evaporation kick independent of bombarding energy is consistent with the Fung and Perlman postulate of constant deposition energy. Since V does not vary with bombarding energy, the graph of η_{11} actually reflects the variation of v_{11} with bombarding energy.

Also plotted in Fig. 10 are the values of η_{11} obtained from the angular-distribution and differential-range measurements and also one other thin-target experiment done especially for this purpose. They are slightly higher than the thick-target values. It has been pointed out[16] that the thin-target experiments give the true average value of η_{11}, $\langle\eta_{11}\rangle$, while the thick-target experiments yield approximately $\langle\eta_{11}R\rangle/\langle R\rangle$, that is η_{11} weighted according to R. Since N is almost unity this is very closely equal to $\langle v_{11}\rangle/\langle V\rangle$, in contrast to $\langle v_{11}/V\rangle$ obtained from thin-target experiments. Using the distribution $P(V)$ from Fig. 8 and $N=1.2$ one calculates that the thin-target average η_{11} should be 1.2 times the thick-target average η_{11}. The two curves in Fig. 10 are separated by just this factor.

DISCUSSION OF PARAMETERS

It must be remembered that the framework for our discussion is the model consisting of a nucleonic cascade

followed by nuclear evaporation. The Monte Carlo calculations described earlier were a detailed arithmetical treatment of the model. The vector analysis may be looked upon as simply a means of parameter fitting consistent with this model. The Turkevich mechanism, to be described later in this section, is a very simplified analytical treatment of the same model. However, the mechanism used by Fung and Perlman,[3] called the single-fast-nucleon mechanism,[8,22] has no obvious a priori justification.

The single-fast-nucleon mechanism assumes that the incident nucleon passes through the nucleus undeviated, but deposits energy E^*. The mechanism is stated analytically in terms of the momentum imparted to the recoil,

$$p_{11}=\frac{2EE^*}{p+(p^2-2EE^*)^{1/2}}. \tag{8}$$

The total energy, momentum, and kinetic energy of the incident particle will be designated E, p, and T, respectively, in this section. (Natural units, c, m_0c, and m_0c^2, are used for velocity, momentum, and energy.) The ratio p_{11}/E^* is plotted in Fig. 12 for two values of E^*. At low bombarding energies the formula reduces to the one used by Fung and Perlman.[3] At high bombarding energies it assumes the simple form

$$p_{11}=(E/p)E^*. \tag{9}$$

Of course, for this mechanism $p_\perp$ is zero.

The mechanism proposed by Turkevich,[23] assumes that the incident nucleon scatters elastically off one nucleon in the nucleus and escapes from the nucleus giving a (P,P') knock-on cascade. The struck nucleon
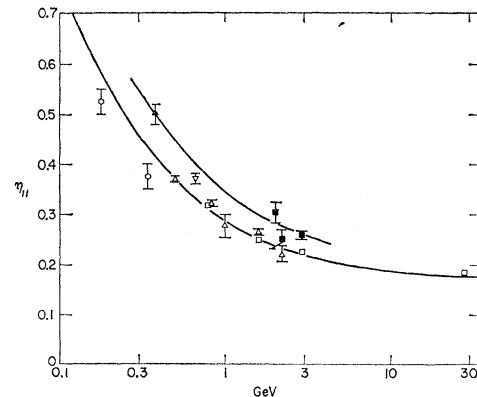

FIG. 10. The values of $\eta_{11}=v_{11}/V$ obtained from thick-target experiments are shown as open symbols, and from thin-target experiments as solid symbols. The curves (see the discussion section) are a factor of 1.2 apart. The symbols are defined as in Fig. 1.

[22] N. A. Perfilov, N. S. Ivanova, O. V. Lozhkin, V. I. Ostrovmov, and V. P. Shamov, Proceedings of the Conference of the Academy of Sciences USSR on the Peaceful Uses of Atomic Energy, July, 1955 [translation by the Consultants Bureau, N. Y. Atomic Energy Commission Report TR-2435, 1956 (unpublished)].
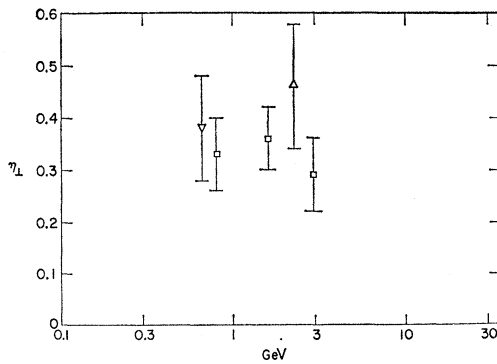
[23] A. Turkevich, quoted in reference 9.

FIG. 11. The values of $\eta_\perp = v_\perp/V$ obtained from the thick-target experiments. The symbols are defined as in Fig. 1.

is captured by the nucleus, converting its kinetic energy, E^*, and momentum, p, into deposition energy, $E^*(A-1)/A$, and recoil momentum, p. The momentum deposited parallel and perpendicular to the beam direction is

$$p_{||} = (1+2/T)^{1/2}E^*, \qquad (10)$$

and

$$p_\perp = [(2/E^*)-1-2/T]^{1/2}E^*. \qquad (11)$$

The first equation is also plotted in Fig. 12 and is of significantly different shape from that of the single-fast-nucleon mechanism. Because of the constancy of V with bombarding energy, the quantity $\eta_{||}$, which is plotted in Fig. 10, is essentially a measure of $v_{||}$, or consequently $p_{||}$. By comparing Figs. 10 and 12 it was found that for constant deposition energy the shape of the Turkevich curve fits the data better than the single-fast-nucleon curve. In fact the two curves drawn a factor of 1.2 apart in Fig. 10 were obtained from Eq. (10) by adjusting one parameter. This parameter, the relative ordinates of the two graphs, $(v_{||}/V)/(p_{||}/E^*)$, was found to be 0.17 for the thick-target data. It is equal to $E^*/27V$. From Fig. 9 it was found that $V=1.32$ (MeV)$^{1/2}$ or 0.0124 in units of c. Thus E^* is approximately 53.5 MeV. That is, one interprets the forward momentum of the recoil as a function of bombarding energy, using the Turkevich mechanism, in terms of a kinetic energy of the struck and captured nucleon of ≈ 53.5 MeV independent of bombarding energy. Taking into account the kinetic energy acquired by the struck nucleus, this leaves ≈ 51.5 MeV as deposition energy. The sum of the binding energies (Q) of the three nucleons to be evaporated is 31.5 MeV, leaving the adequate amount of 20 MeV for the sum of the kinetic energies of the three particles plus the evaporation recoil, and for gamma de-excitation.

So far, we have considered only the collision of the bombarding particle with a stationary nucleon in the nucleus. The effect of the Fermi motion will cause a distribution in the momentum of the recoil but will not add to the deposition energy if the struck particle is subsequently captured. Thus, we are attempting to broaden the Turkevich model to consider quasi-elastic

scattering. In the limit of high energies, as we have said before, the hole momentum should contribute mainly to V. However, even for an isotropic momentum distribution of the target nucleon, Eqs. (10) and (11) may not give the correct relationship between the average values of $p_{||}$ or $p_\perp$ and the average deposition energy. Neglecting this effect because of its complexity, we conclude that the magnitude of V should result from the evaporation of three nucleons with a total of 20 MeV of kinetic energy plus the hole momentum arising from the struck nucleon. Let us estimate the hole momentum, V_H, by calculating the evaporation kick, V_E, and subtracting it from the total observed V. The average velocity imparted to the recoil due to the evaporation process can be obtained from the following equation:

$$V_E{}^2 = \frac{2X^2}{n}\left\{\frac{[E^*(A-1)/A+Q-E_\gamma]}{A_R{}^2}\right\}$$

$$\times \left\{\frac{A_R+\frac{1}{2}(n-1)}{A_R+\frac{1}{2}(n+1)}\right\}. \qquad (12)$$

The quantity A_R is the mass of the recoil. The energy dissipated by gamma emission E_γ will be assumed to be 5 MeV. The number of particles evaporated, n, is three on this model. The quantity X is a number from random walk theory which approaches $n^{1/2}$ for large n, but for three particles is equal[24] to 13/8. The equation assumes that the Coulomb barrier is small and that all the particles cause equal decrements in the available energy. The last term in brackets approximately takes account of the changing mass of the recoil during the evaporation process. Putting in the above numbers one estimates V_E to be 0.0069. Then using the equation[24] for summing two random vectors, $V = (3V_H{}^2 + V_E{}^2)/3V_H$, one obtains the contribution to V due to the hole, $V_H = 0.0107$. This is larger than V_E meaning that most of the observed V comes from the hole momentum and not the evaporation kick. The energy of the struck nucleon before collision which gave rise to this V_H is given by $(27)^2 V_H{}^2/2$, or 39
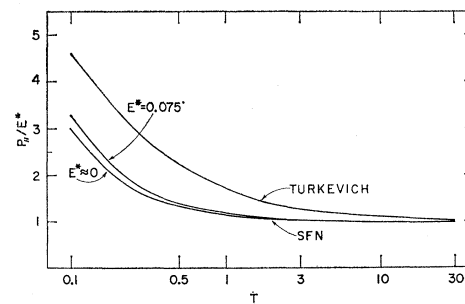

FIG. 12. The predictions of the Turkevich and single-fast-nucleon mechanisms for the ratio of the momentum deposited along the beam direction to the deposition energy as a function of bombarding energy. The unit of energy is the nucleon mass.

[24] C. Hsiung, H. Hsiung, and A. A. Gordus, J. Chem. Phys. 34, 535 (1961).

MeV. Even if one assumed this nucleon were at the top of the Fermi sea this would give a total well depth of 47 MeV, which appears to be a little large. However in the light of the extremely simple mechanism used to make this analysis, and our present knowledge of nuclear potentials, the result may not indicate any real inconsistency. If, in explaining the magnitude of V we were to assume a deuteron were evaporated instead of two nucleons, we would only need a kinetic energy of the struck nucleon before collision of 22 MeV. Thus a small proportion of deuteron emission would lower the average value somewhat. If the value of the range-velocity exponent N had been taken as 1.0 instead of 1.2, the deposition energy would have been raised by only 3 MeV and the energy of the struck nucleon lowered by 3 MeV.

Till now we have been discussing only the average value of V. To see if the distribution of V as shown in Fig. 8 is consistent with this simple picture, a Monte Carlo calculation similar to the evaporation calculation described earlier was performed. The distribution of recoil momenta resulting from a 39-MeV hole plus the evaporation of three nucleons from Al^{27} with an excitation of 51.5 MeV was calculated and plotted as the curve in Fig. 8. The agreement is reasonable.

Thus, the Turkevich mechanism appears to be able to account for the variation of v_{11} with bombarding energy, and approximately for the magnitude and distribution of V. However, there is one important piece of information inconsistent with the present mechanism. Equation (11) would predict values of $\eta_\perp$ of about 1.1 where Fig. 11 indicates values of 0.35. In other words, the Turkevich mechanism for low deposition energies predicts that the recoil should travel at almost 90° to the incident beam. Both the thick-target measurements and the angular-distribution measurements are inconsistent with such large values of the sidewise knock-on kick. This type of effect, sideways peaking of the knock-on product, is also predicted by the Monte Carlo calcu-lations. Thus, both forms of the basic model predict behavior which is not observed experimentally. Of course, this discrepancy makes the previous conclusions using the Turkevich mechanism suspect. However it is still amazing that such a simple mechanism was able to correlate as much of the data as it did. One should also note that in the Turkevich mechanism the mass of the struck nucleus is 27, which is in sharp contrast to the predictions of the Monte Carlo calculations shown in Table IV.

One last point to be discussed is the value obtained for the parameter b/a which indicated a slight negative anisotropy of the angular distribution of the evaporation kick in the system of the struck nucleus. Halpern[25] has proposed a mechanism to explain the same type of effect in fission induced by high-energy particles which is essentially an extension of the Turkevich mechanism to include angular-momentum effects. He points out that the effect should be most pronounced when one singles out the cases of low deposition energy as we are doing here. The anisotropy of V may also be caused by that part which arises from hole momentum. That is, if the collision preferentially occurs in a region of the nucleus where the struck nucleon was moving preferentially perpendicular to the incident beam, then one will get negative anisotropy.

[25] I. Halpern, Nucl. Phys. 11, 522 (1959).